

Wigner-Mott scaling of transport near the two-dimensional metal-insulator transition

M. M. Radonjić,¹ D. Tanasković,¹ V. Dobrosavljević,² K. Haule,³ and G. Kotliar³

¹*Scientific Computing Laboratory, Institute of Physics Belgrade, University of Belgrade, Pregrevica 118, 11080 Belgrade, Serbia*

²*Department of Physics and National High Magnetic Field Laboratory, Florida State University, Tallahassee, Florida 32306, USA*

³*Department of Physics and Astronomy, Rutgers University, Piscataway, New Jersey 08854, USA*

Electron-electron scattering usually dominates the transport in strongly correlated materials. It typically leads to pronounced resistivity maxima in the incoherent regime around the coherence temperature T^* , reflecting the tendency of carriers to undergo Mott localization following the demise of the Fermi liquid. This behavior is best pronounced in the vicinity of interaction-driven (Mott-like) metal-insulator transitions, where the T^* decreases, while the resistivity maximum ρ_{max} increases. Here we show that, in this regime, the entire family of resistivity curves displays a characteristic scaling behavior $\rho(T)/\rho_{max} \approx F(T/T_{max})$, while the ρ_{max} and $T_{max} \sim T^*$ assume a powerlaw dependence on the quasi-particle effective mass m^* . Remarkably, precisely such trends are found from an appropriate scaling analysis of experimental data obtained from diluted two-dimensional electron gases in zero magnetic fields. Our analysis provides strong evidence that inelastic electron-electron scattering – and not disorder effects – dominates finite temperature transport in these systems, validating the Wigner-Mott picture of the two-dimensional metal-insulator transition.

PACS numbers: 71.27.+a, 71.30.+h, 72.10.-d

I. INTRODUCTION

The physical nature of scattering processes which control transport represents one of the most fundamental properties for any material. At the lowest temperatures the thermal excitations are few, and elastic impurity scattering dominates. Raising the temperature introduces two basic pathways to modify transport. First, elastic scattering can acquire a temperature dependence either through the modified screening of the impurity potential, or through dephasing processes.^{1,2} This general mechanism encapsulates the physical content of all “quantum corrections” – both in the diffusive and the ballistic regime – predicted within the Fermi liquid framework. Indeed, careful and precise experiments have confirmed the validity of this physical picture for many good metals with weak disorder.¹ Physically, it relies on the existence of long-lived quasiparticles within a degenerate electron gas.

The second route comes into play in instances where correlation effects due to electron-electron interactions are significant. Here, the Fermi liquid regime featuring degenerate quasiparticles is often restricted to a very limited temperature range $T \ll T^* \ll T_F$, well below the “coherence temperature” T^* , which itself is much smaller than the Fermi temperature T_F . In such materials, which include rare-earth intermetallics,^{3,4} many transition metal oxides,⁵ and several classes of organic Mott systems,⁶⁻⁸ a broad intermediate temperature regime emerges $T \sim T^* \ll T_F$ where *inelastic* electron-electron scattering dominates all transport properties. Such scattering directly reflects the thermal destruction of Landau quasiparticles – a situation describing the demise of a coherent Fermi liquid. In these materials, in the rele-

vant temperature range, the electron-phonon scattering is much weaker than the electron-electron one.

When a material is tuned to the vicinity of any metal-insulator transition,⁹ both disorder and electron-electron interactions are of *a priori* importance. But which of these two scattering mechanisms – elastic or inelastic – dominates the experimentally relevant temperature range? Answering this question should provide important clues as to which of the localization mechanisms dominate in any given material. Unfortunately, experimental systems permitting sufficiently precise tuning of control parameters are generally rather few. An attractive class of systems where a dramatic metal to insulator crossover is observed in a narrow parameter range is provided by two dimensional electron gases (2DEG), such as silicon MOSFETs or GaAs/AlGaAs heterostructures.¹⁰⁻¹² One of the most striking features observed in these systems is the pronounced resistivity drop on the metallic side of the transition. While conventional, relatively weak temperature dependence is found at high densities ($n \gg n_c$), very strong temperature dependence is found near the critical density n_c , roughly in the same density range $n_c \lesssim n \lesssim 2n_c$ where other strong correlation phenomena were observed, e.g. large m^* enhancement.¹³ Here, pronounced resistivity maxima are observed at $T \sim T_{max}(n)$, followed by a dramatic resistivity drop at lower temperatures, whose physical origin remains a subject of much controversy and debate.¹⁰⁻¹²

In this paper we argue that the electron-electron scattering dominates the transport in a broad concentration and temperature range on the metallic side of the metal-insulator transition (MIT) in Si MOSFETs and GaAs/AlGaAs heterostructures. This conclusion is

reached by: (i) A detailed scaling analysis of the metallic resistivity curves; (ii) Establishing a similarity in the transport properties of the 2DEG and well-studied strongly correlated materials near the interaction-driven MIT; (iii) Making a comparison of the resistivity curves in 2DEG with those in a simple model of the Mott MIT. Our conclusions favor the interaction-driven (Wigner-Mott) scenario^{14–18} of the MIT in 2DEG and provide a guidance for the development of a microscopical theory of incoherent transport in diluted 2DEG.

The remaining part of the paper is organized as follows. Our phenomenological scaling of the experimental data is shown in Sec. II, and the analogy with strongly correlated three dimensional (3D) materials is highlighted in Sec. III. The scaling analysis in a simple model of the Mott MIT is presented in Sec. IV, and Sec. V contains the conclusion and discussion.

II. SCALING ANALYSIS OF THE RESISTIVITY MAXIMA

The experimental data reveal well defined trends in the density dependence of the resistivity maxima, suggesting a scaling analysis. While many different scenarios for the metal-insulator transition predict some form of scaling, its precise features may provide clues to what mechanism dominates the transport.

All of the curves displaying a resistivity maximum have an almost identical shape [Fig. 1], strongly suggesting that unique physical processes are responsible for a strong temperature dependence of the resistivity

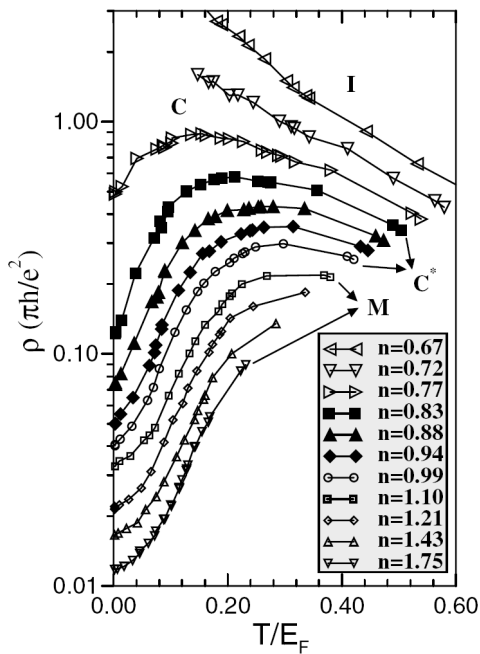


FIG. 1: Resistivity as a function of temperature from the experiments on Si MOSFET by Pudalov *et al.* (Ref. 19).

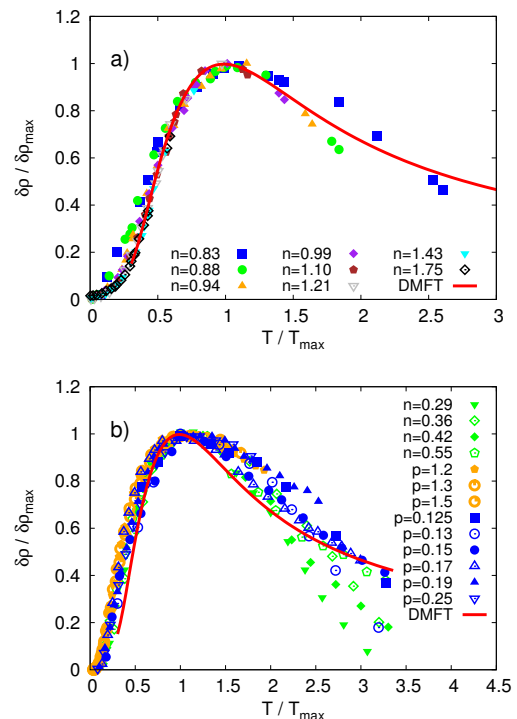


FIG. 2: (Color online) Scaled resistivity as a function of scaled temperature for different electron (hole) concentrations, for Si MOSFET (a) and GaAs heterostructures (b). The experimental data are taken from Ref. 21 (MOSFETs), Ref. 23 (p-GaAs/AlGaAs, blue symbols), Ref. 24 (n-GaAs/AlGaAs, green symbols), and Ref. 25 (p-GaAs, orange symbols). The solid line is the scaling function obtained for a simple model of the MIT (see Sec. IV).

in a large range of concentrations. The resistivity maxima are typically observed at temperatures comparable to the Fermi temperature, where a physical picture of long-lived quasiparticles is no more valid. Complementary experiments^{11,13} on the same material have revealed that large effective mass m^* enhancements are observed in the same density range. This behavior is a clear signature of strong correlation effects which, in all known examples, produce very strong inelastic electron-electron scattering in the appropriate temperature range. The electron-phonon scattering is negligibly small for $T < T_F \lesssim 10$ K.²⁰ Since a strongly correlated system is typically characterized by a single characteristic energy scale $T^* \sim (m/m^*)T_F$, we expect the scaling function $f(x)$ to assume a universal form, while the scaling parameters $T_{max} \equiv T^*$ and ρ_{max} to assume a simple, power-law dependence on the effective mass m^* . Guided by these observations, in this Section we introduce a scaling ansatz and perform a scaling analysis of the resistivity curves in Si MOSFETs and GaAs heterostructures.

A. Phenomenological scaling hypothesis

In accordance to what is typically found in other examples of strongly correlated metals with weak to moderate disorder,⁶ we expect the resistivity to assume an additive form, $\rho(T) = \rho_o + \delta\rho(T)$. Here, ρ_o is the residual resistivity due to impurity scattering, and the temperature-dependent contribution $\delta\rho(T)$ is expected to be dominated by inelastic electron-electron scattering. Based on these general considerations, we propose that the temperature-dependent term assumes a scaling form

$$\delta\rho(T) = \delta\rho_{max} f(T/T_{max}), \quad (2.1)$$

where $\delta\rho_{max} = \rho_{max} - \rho_o$.

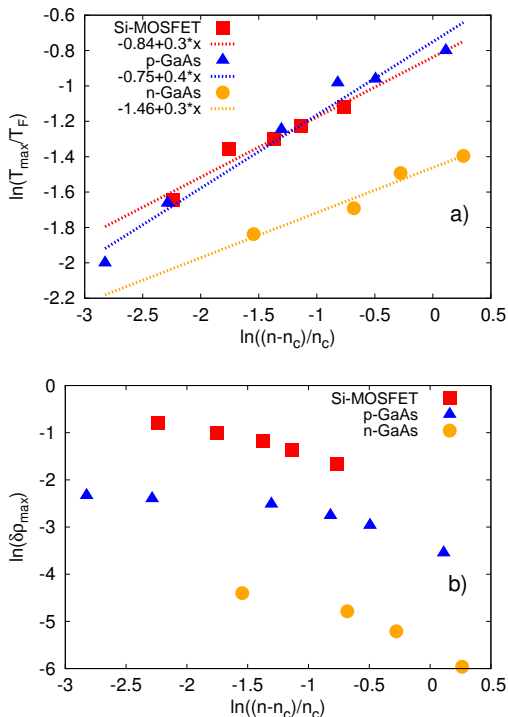


FIG. 3: (Color online) T_{max} normalized to Fermi temperature (a), and maximal resistivity $\delta\rho_{max} = \rho_{max} - \rho_o$ in units $\pi\hbar/e^2$ (b), as a function of a reduced density. The data are taken from Refs. 21,23,24.

To test this phenomenological scaling hypothesis, we perform a corresponding analysis of experimental data in several systems displaying 2D-MIT. We start with the Si MOSFET data¹⁹ analyzed in Ref. 21. We concentrate on metallic curves below the separatrix C. In the range of concentrations, $0.83 < n < 1.10$, the resistivity curves have a clear maximum, and nicely collapse with the proposed scaling ansatz, Fig. 2(a). In fact, we can use the scaling ansatz to collapse also the data for $1.21 < n < 1.75$, where T_{max} and ρ_{max} are determined from the least square fit to the scaling curve. Clearly all eight resistivity curves belong to the same family (have the same functional form), and thus must be explained by

a single dominant transport mechanism. This conclusion is even more convincing if we apply the same analysis to several different materials, including an ultra high mobility GaAs sample, Fig. 2(b). While the diffusive physics cannot possibly apply in such a broad parameter range, we see that the scaling form we propose proves to be an extremely robust feature of all available 2D-MIT systems. This result is very significant, because disorder effects must be significantly weaker in these ultra-clean materials, while the interaction effects are expected to be even stronger.

B. Critical behavior of the Wigner-Mott scaling

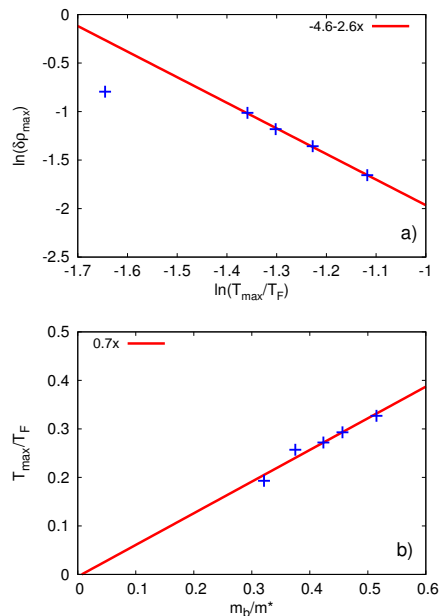


FIG. 4: (Color online) (a) Maximum resistivity $\delta\rho_{max} = \rho_{max} - \rho_o$ as a function of T_{max} . (b) T_{max} as a function of inverse effective mass m^* . m_b is the band mass in Si MOSFETs. The data are taken from Refs. 21 and 26.

Having demonstrated data collapse, we are now in a position to examine the critical behavior of the relevant crossover scale. We thus examine the behavior of T_{max} and ρ_{max} as a function of reduced concentration $(n - n_c)/n_c$ and effective mass m^* (as determined by complementary experiments).

For different realizations of 2DEG, T_{max} shows approximately power law dependence on the reduced concentration [Fig. 3(a)] and even the exponents are similar. T_{max} in our physical picture has a clear physical interpretation as a coherence temperature - the temperature when the inelastic electron-electron scattering time becomes comparable to \hbar/E_F , leading to incoherent transport. The resistivity maximum, however, shows less universal form. It varies a lot in different physical systems. This does not come as a surprise since the resistivity shows nonuniver-

sal features also in three dimensional strongly correlated materials near the Mott transition. We discuss in detail the analogy with the Mott systems in Secs. III and IV.

In a Si MOSFET the resistivity maximum $\delta\rho_{max} = \rho_{max} - \rho_0$ shows power law dependence on T_{max} in a fairly broad concentration range [Fig. 4(a)]. We further analyze the critical behavior for Si MOSFET using the data for the effective mass as determined by Shashkin *et al.*¹³ from magnetoresistance measurements in a parallel magnetic field. We find that T_{max} is inversely proportional to the effective mass m^* . This behavior is typical to all systems near the Mott MIT, where the coherence temperature is inversely proportional to the effective mass, as a landmark of strong correlations.

C. Breakdown of the diffusion mode scaling

We have successfully collapsed resistivity curves in a broad temperature and concentration range and for several physical realizations of 2DEG. The physical picture behind the proposed scaling is that the 2D MIT is an interaction-driven (Wigner-Mott) MIT,^{14–18} and that the dominant temperature dependence in the resistivity originates from strong electron-electron scattering. Another proposed scenario envisions disorder as the principal driving force for localization,^{21,22} while the interactions are most important above the critical density and at low temperatures, where they suppress the tendency to localization. An appropriate theory, based on a Fermi liquid framework,²¹ has predicted that a resistivity maximum should be observed on the metallic side, with the resistivity assuming the scaling form

$$\rho(T)/\rho_{max} = f[\rho_{max} \ln(T/T_{max})]. \quad (2.2)$$

Here $f(x)$ is a universal scaling function predicted by theory. The authors point out, though, that this prediction is expected to be valid only within the diffusive regime, where the thermal energy $k_B T$ is smaller than the

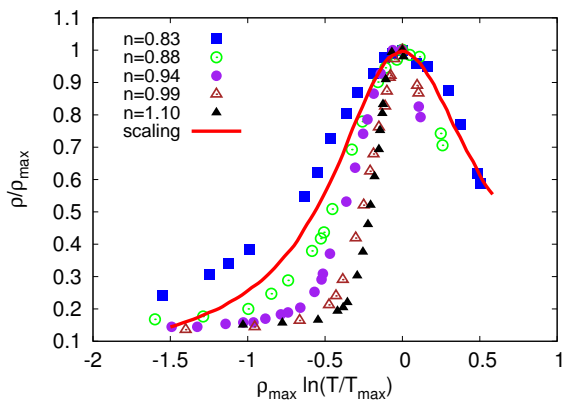


FIG. 5: (Color online) Resistivity as a function of temperature scaled as in Ref.²¹. Red solid line is the calculated scaling curve.

elastic scattering rate \hbar/τ . According to this picture, a different (ballistic) mechanism for transport is expected outside the diffusive regime, presumably leading to a different temperature dependence, so the proposed scaling no longer holds. This analysis was applied to the experimental data of Ref.19, but was accordingly restricted to only three densities closest to the transition. Indeed, if the scaling formula is applied in a broader range of concentrations, the resistivity curves clearly do not collapse [Fig. 5]. While the Fermi liquid renormalization group calculations are very important in order to answer a fundamental question of necessary conditions for a true MIT at zero temperature, our analysis emphasizes that the understanding of various diluted 2DEG in a broad range of parameters requires the physics beyond the conventional Fermi liquid framework.

III. SCALING IN 3D MATERIALS

The strong temperature dependence of resistivity is a well known feature of many strongly correlated materials. A pronounced resistivity maximum is observed in heavy fermions,^{3,4} and charge-transfer organic salts,^{6–8} where the correlation strength is tuned by applying an external pressure. The essential mechanism of transport in these materials relies on strong inelastic electron-electron scattering, and the Fermi liquid behavior is restricted to

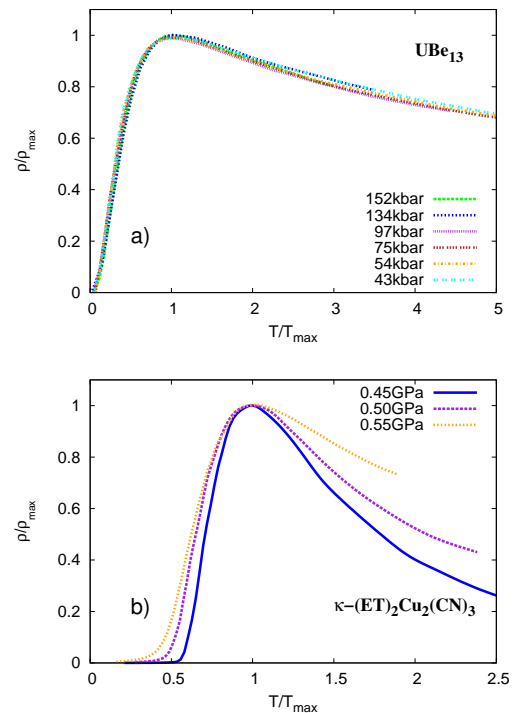


FIG. 6: (Color online) Scaled resistivity curves for UBe_{13} (a) and $\kappa-(ET)_2Cu_2(CN)_3$ (b), for different external pressure. The data are taken from Refs. 4 and 7.

the lowest temperatures. As the temperature increases, the electron mean free path becomes comparable to, or smaller than the lattice spacing, and the transport becomes incoherent. The electron-phonon scattering is here much weaker than the electron-electron one. The temperature of the resistivity maximum can be taken as a definition of the coherence temperature T^* . It is inversely proportional to the effective mass, and much smaller than the bare Fermi temperature, $T^* \sim (m_b/m^*)T_F$. The same scaling ansatz as given by Eq. (2.1) was used to collapse the resistivity curves for CeCu₆ already in an early paper by Thompson and Fisk.³

Here we illustrate the similarity in transport properties of these systems and 2DEG by scaling the resistivity data for heavy fermion UBe₁₃ from Ref. 4 [Fig. 6(a)], and for a charge-transfer conductor κ -(ET)₂Cu₂(CN)₃ [Fig. 6(b)]. The collapse of the resistivity curves is excellent for UBe₁₃, and well-defined trends are seen in κ -(ET)₂Cu₂(CN)₃. Remarkable similarity in resistivity curves in such diverse physical systems like Si MOSFETs, GaAS heterostructures, heavy fermions and charge-transfer organic conductors is, in our view, a manifestation of the same physical processes in the vicinity of the interaction-driven MIT.

IV. SCALING IN THE MICROSCOPIC MODEL OF THE INTERACTION-DRIVEN MIT

Having phenomenologically established precise and well defined scaling behavior of the experimental curves on the metallic side of the 2D MIT for temperatures near T^* , we now address its microscopic origin. More precisely, we would like to understand just how robust this result is. Does it depend on subtle details describing the interplay of disorder and interactions of 2DEG materials, as suggested in Ref. 27, or is it a generic feature of strong correlation near interaction-driven MIT. To answer this important question we deliberately focus on the simplest microscopic model for interaction-driven MIT: The clean single-band Hubbard model at half-filling. Accurate and quantitatively precise results can be obtained for temperature-dependent transport for this model within the DMFT approximation.²⁸ While the DMFT reproduces Fermi liquid behavior at the lowest temperatures, it is particularly useful in the studies of "high temperature" incoherent transport. Results of such calculation, obtained by the Continuous Time Quantum Monte Carlo (CTQMC) impurity solver^{29,30} followed by the analytical continuation by the Maximum Entropy Method³¹, can be analyzed using precisely the same scaling procedure we proposed for experimental data. We concentrate on the metallic phase of the Hubbard model with the interaction parameter U smaller than the value at the critical end-point U_c . The resistivity curves [Fig. 7(a)] have qualitatively the same form as in 2DEG. The resistivity sharply increases with temperature, reaches a maximum and then decreases. The temperature of resistivity maximum

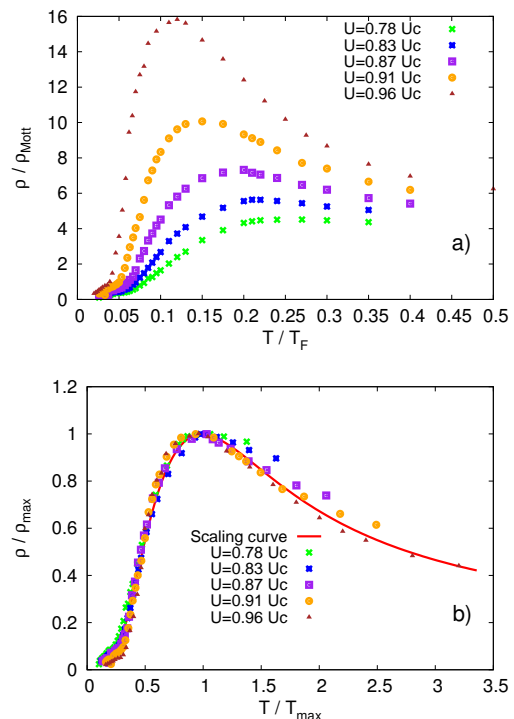


FIG. 7: (Color online) (a) Resistivity as a function of temperature for several interaction strengths in the half-filled Hubbard model solved within the DMFT. The resistivity is normalized to the Mott limit value, which corresponds to the scattering length of one lattice spacing. (b) Scaled resistivity curves.

imum decreases as the system approaches the MIT.

Most remarkably, precisely the same scaling form as in 2DEG is found to describe all resistivity curves close to the Mott transition [Fig. 7(b)]. In addition, we find that the scaling parameters T_{max} and ρ_{max} again display a power law dependence on the effective mass [Fig. 8], and even the exponents are similar. Finally, we contrast the DMFT scaling function with that obtained from 2DEG experiments. We find surprisingly accurate agreement between the DMFT prediction for the scaling function $f(x)$ and experimental data on all available materials [Fig. 2]. We emphasize, however, that our scaling hypothesis is valid only in the metallic phase for $U < U_c$ and for temperatures comparable to $T^* \sim 1/m^*$. It should be contrasted with the scaling near the critical end-point (U_c, T_c) ,^{32,33} or the proposed quantum critical scaling in the high-temperature regime above the critical end-point.³⁴

We should point out that for this model, the proposed resistivity scaling is not valid at the lowest temperatures $T \ll T_{max}$, deep within the Fermi liquid region: According to the Kadowaki-Woods relation, here $\rho \approx AT^2$ where $A \sim 1/m^{*2} \sim 1/T_{max}^2$, and the scaling is violated if the resistivity is scaled by ρ_{max} . For $T \gtrsim 0.3T_{max}$ the collapse of the resistivity curves is excellent, [Fig. 7(b)], and we define the DMFT scaling curve for this temper-

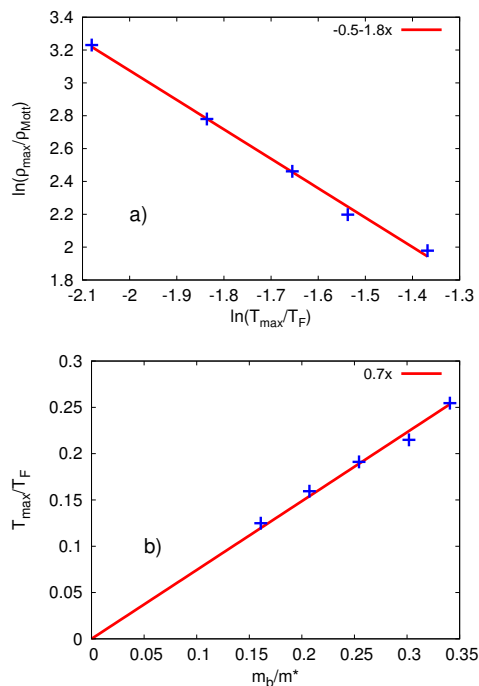


FIG. 8: (Color online) (a) Maximum resistivity as a function of the corresponding temperature from the DMFT solution of the Hubbard model. (b) T_{\max} as a function of the inverse effective mass.

ature range. This is also the reason for the deviations in the scaling in Fig. 6(b) for κ -organics, the materials whose properties are described remarkably well within the Hubbard model.^{6,8} In the Anderson lattice model, on the other hand, the resistivity maximum does not change much near the MIT and it saturates approximately to the value which corresponds to the scattering length of one lattice spacing (Mott limit). In this case our scaling ansatz is valid in the whole temperature range up to $T = 0$,³⁶ and the collapse of the resistivity curves seen in the experiments is excellent [Fig. 6(a)].

Microscopic theory of the 2DEG should also include nonlocal correlations which are neglected in a simple DMFT approach. A more realistic extended Hubbard model displays a two-stage Wigner-Mott localization.^{17,18} The metal-insulator transition in this model is found in the region with already developed nonlocal charge correlations. In the immediate critical regime, the critical behavior can be represented by an effective Hubbard model, partially justifying the success of the present modeling. The existence of a coherence scale T^* which vanishes at the onset of charge order is also found in the 2D extended Hubbard model solved by finite- T Lanczos diagonalization.³⁵ This result is relevant for quarter-filled layered organic materials, which further supports the importance and generality of the ideas presented here.

V. CONCLUSION AND DISCUSSION

In this paper we argued that the emergence of resistivity maxima upon thermal destruction of heavy Fermi liquids should be regarded as a generic phenomenon in strongly correlated systems. We demonstrated that the resulting family of resistivity curves typically obeys a simple phenomenology displaying scaling behavior. Our detailed model calculations show that all of the qualitative and even quantitative features of this scaling phenomenology are obtained from a microscopic model of heavy electrons close to the Mott metal-insulator transition. We should stress, however, that the proposed scaling behavior obtains - both in our theory and in experiments - only within the metallic regime not too close to the transition and the temperature regime around the resistivity maxima. In contrast, earlier experiments focused on the immediate vicinity of the metal-insulator transition, where different "quantum critical" scaling was found.^{10,37-39} Remarkably, precisely such behavior was also found in very recent studies of quantum critical transport near interaction-driven transitions,³⁴ but this was identified in a different parameter regime than the one studied in the present paper.

Our results provide compelling evidence that several puzzling aspects of transport in low density two-dimensional electron gases in zero magnetic fields can be understood and explained within the Wigner-Mott scenario of strong correlation.¹⁴⁻¹⁸ This physical picture views the strong correlation effects in the low density 2DEG as the primary driving force behind the transition, and additional disorder effects as less significant, secondary processes. In the Wigner-Mott picture the insulator essentially consists of interaction-localized magnetic moments. Remarkably, the magneto-capacitance measurements of Prus *et al.*²⁶ show that the behavior characteristic of localized magnetic moments, $\chi(T)/n \approx g\mu_B^2/T$, is seen near the critical density, while only weak Pauli-like temperature dependence was observed at higher density. Very recent experiments on Si MOSFETs find that the thermopower diverges near the MIT.⁴⁰ The authors argue that divergence of the thermopower is not related to the degree of disorder and reflects the divergence of the effective mass at a disorder-independent density, behavior that is typical in the vicinity of an interaction-induced phase transition. Additional hints supporting this physical picture of 2D MIT are provided by existing first principle Quantum (diffusion) Monte Carlo results for the low density 2DEG of Ceperley⁴¹ and others.^{27,42,43} These calculations find that the correlated metallic state has an "almost crystalline" structure, thus having a very strong short range charge-order (as seen, for example, in the density correlation function).

Within the physical picture that we propose, the inelastic electron-electron scattering takes central stage,^{44,45} in contrast to disorder-dominated scenarios, where the interaction effects mainly introduce the temperature dependence of *elastic* electron-impurity

scattering.² The two physical pictures describe two completely different scattering processes, which are expected to be of relevance in complementary but in essentially non-overlapping parameter regimes. Indeed, inelastic scattering dominates only outside the coherent Fermi-liquid regime, which in good metals happens only at fairly high temperatures. In strongly correlated regimes that we consider, the situation is different. Here the Fermi liquid coherence is found only at very low temperatures $T < T^* \ll T_F$, behavior which is generally observed in all system with appreciable effective mass enhancement. The results presented in this paper provide precise and detailed characterization of this incoherent regime, revealing remarkable coincidence of trends observed in the experiment to those found from the Wigner-Mott picture of the interaction-driven metal-insulator transition. Our scaling ansatz is proposed based on the physical arguments and the experimental data. While consistent with simple model calculations for strongly correlated electronic systems, our work does not directly address specific microscopic mechanism responsible for current dissipation,

a process that in 2DEG systems should be facilitated by impurities and imperfections.⁴⁵ Still, it provides very strong motivation to develop a more realistic microscopic theory of incoherent transport in the strongly correlated regime of diluted 2DEG. This important task remains a challenge for future work.

Acknowledgments

The authors thank A. Punnoose and A. M. Finkelstein for usefull discussions. D.T. and M.M.R. acknowledge support from the Serbian Ministry of Education and Science under project No. ON171017. V.D. was supported by the National High Magnetic Field Laboratory and the NSF Grant No. DMR-1005751, G.K. by the NSF Grant No. DMR-0906943, and K.H. by the NSF Grant No. DMR-0746395. Numerical simulations were run on the AEGIS e-Infrastructure, supported in part by FP7 projects EGI-InSPIRE, PRACE-IIP and HP-SEE.

-
- ¹ P. A. Lee and T. V. Ramakrishnan, *Rev. Mod. Phys.* **57**, 287 (1985).
² G. Zala, B. N. Narozhny, and I. L. Aleiner, *Phys. Rev. B* **64**, 214204 (2001).
³ J. D. Thompson and Z. Fisk, *Phys. Rev. B* **31**, 389 (1985).
⁴ M. W. McElfresh, M. B. Maple, J. O. Willis, Z. Fisk, J. L. Smith, and J. D. Thompson, *Phys. Rev. B* **42**, 6062 (1990).
⁵ M. M. Qazilbash, K. S. Burch, D. Whisler, D. Shrekenhamer, B. G. Chae, H. T. Kim, and D. N. Basov, *Phys. Rev. B* **74**, 205118 (2006).
⁶ P. Limelette, P. Wzietek, S. Florens, A. Georges, T. A. Costi, C. Pasquier, D. Jérôme, C. Mézière, and P. Batail, *Phys. Rev. Lett.* **91**, 016401 (2003).
⁷ Y. Kurosaki, Y. Shimizu, K. Miyagawa, K. Kanoda, and G. Saito, *Phys. Rev. Lett.* **95**, 177001 (2005).
⁸ J. Merino, M. Dumm, N. Drichko, M. Dressel, and R. H. McKenzie, *Phys. Rev. Lett.* **100**, 086404 (2008).
⁹ N. F. Mott, *Metal-Insulator Transition* (Taylor & Francis, London, 1990).
¹⁰ E. Abrahams, S. V. Kravchenko, and M. P. Sarachik, *Rev. Mod. Phys.* **73**, 251 (2001).
¹¹ S. V. Kravchenko and M. P. Sarachik, *Rep. Prog. Phys.* **67**, 1 (2004).
¹² B. Spivak, S. V. Kravchenko, S. A. Kivelson, and X. P. A. Gao, *Rev. Mod. Phys.* **82**, 1743 (2010).
¹³ A. A. Shashkin, S. V. Kravchenko, V. T. Dolgoplov, and T. M. Klapwijk, *Phys. Rev. B* **66**, 073303 (2002).
¹⁴ J. S. Thakur and D. Neilson, *Phys. Rev. B* **59**, R5280 (1999).
¹⁵ B. Spivak, *Phys. Rev. B* **64**, 085317 (2001).
¹⁶ S. Pankov and V. Dobrosavljević, *Phys. Rev. B* **77**, 085104 (2008).
¹⁷ A. Camjayi, K. Haule, V. Dobrosavljevic, and G. Kotliar, *Nature Phys.* **4**, 932 (2008).
¹⁸ A. Amaricci, A. Camjayi, K. Haule, G. Kotliar, D. Tanasković, and V. Dobrosavljević, *Phys. Rev. B* **82**, 155102 (2010).
¹⁹ V. M. Pudalov, G. Brunthaler, A. Prinz, and G. Bauer, *Physica E* **3**, 79 (1998).
²⁰ T. Ando, A. B. Fowler, and F. Stern, *Rev. Mod. Phys.* **54**, 437 (1982).
²¹ A. Punnoose and A. M. Finkelstein, *Phys. Rev. Lett.* **88**, 016802 (2001).
²² A. R. Hamilton, M. Y. Simmons, M. Pepper, E. H. Linfield, and D. A. Ritchie, *Phys. Rev. Lett.* **87**, 126802 (2001).
²³ Y. Hanein, U. Meirav, D. Shahar, C. C. Li, D. C. Tsui, and H. Shtrikman, *Phys. Rev. Lett.* **80**, 1288 (1998).
²⁴ M. P. Lilly, J. L. Reno, J. A. Simmons, I. B. Spielman, J. P. Eisenstein, L. N. Pfeiffer, K. W. West, E. H. Hwang, and S. Das Sarma, *Phys. Rev. Lett.* **90**, 056806 (2003).
²⁵ X. P. A. Gao, G. S. Boebinger, A. P. Mills, A. P. Ramirez, L. N. Pfeiffer, and K. W. West, *Phys. Rev. Lett.* **94**, 086402 (2005).
²⁶ O. Prus, Y. Yaish, M. Reznikov, U. Sivan, and V. Pudalov, *Phys. Rev. B* **67**, 205407 (2003).
²⁷ G. Fleury and X. Waintal, *Phys. Rev. B* **81**, 165117 (2010).
²⁸ A. Georges, G. Kotliar, W. Krauth, and M. J. Rozenberg, *Rev. Mod. Phys.* **68**, 13 (1996).
²⁹ P. Werner, A. Comanac, L. de Medici, M. Troyer, and A. J. Millis, *Phys. Rev. Lett.* **97**, 076405 (2006).
³⁰ K. Haule, *Phys. Rev. B* **75**, 155113 (2007).
³¹ T. Maier, M. Jarrell, T. Pruschke, and M. H. Hettler, *Rev. Mod. Phys.* **77**, 1027 (2005).
³² G. Kotliar, E. Lange, and M. J. Rozenberg, *Phys. Rev. Lett.* **84**, 5180 (2000).
³³ P. Limelette, A. Georges, D. Jérôme, P. Wzietek, P. Metcalf, and J. M. Honig, *Science* **302**, 89 (2003).
³⁴ H. Terletska, J. Vučićević, D. Tanasković, and V. Dobrosavljević, *Phys. Rev. Lett.* **107**, 026401 (2011).
³⁵ L. Cano-Cortés, J. Merino, and S. Fratini, *Phys. Rev. Lett.* **105**, 036405 (2010).
³⁶ D. Tanasković, K. Haule, G. Kotliar, and V. Dobrosavljević, *Phys. Rev. B* **84**, 115105 (2011).
³⁷ S. V. Kravchenko, W. E. Mason, G. E. Bowker, J. E.

- Furieux, V. M. Pudalov, and M. D'Iorio, *Phys. Rev. B* **51**, 7038 (1995).
- ³⁸ D. Popović, A. B. Fowler, and S. Washburn, *Phys. Rev. Lett.* **79**, 1543 (1997).
- ³⁹ V. Dobrosavljević, E. Abrahams, E. Miranda, and S. Chakravarty, *Phys. Rev. Lett.* **79**, 455 (1997).
- ⁴⁰ A. Mokashi, S. Li, Bo Wen, S. V. Kravchenko, A. A. Shashkin, V. T. Dolgoplov, M. P. Sarachik, preprint arXiv:1111.7238 (2011).
- ⁴¹ D. M. Ceperley and B. J. Alder, *Phys. Rev. Lett.* **45**, 566 (1980).
- ⁴² S. T. Chui and B. Tanatar, *Phys. Rev. Lett.* **74**, 458 (1995).
- ⁴³ X. Waintal, *Phys. Rev. B* **73**, 075417 (2006).
- ⁴⁴ M. C. Aguiar, E. Miranda, V. Dobrosavljević, E. Abrahams, and G. Kotliar, *Europhys. Lett.* **67**, 226 (2004).
- ⁴⁵ A. V. Andreev, S. A. Kivelson, and B. Spivak, *Phys. Rev. Lett.* **106**, 256804 (2011).